

Focused Ultrasound Blood – Brain Barrier Opening Alters the Murine Microbiome

Alina R. Kline - Schoder
Dept. of Biomedical Engineering
Columbia University
New York, NY USA
ark2173@columbia.edu

Jonas Bendig
Dept. of Biomedical Engineering
Columbia University
New York, NY USA
jb4781@columbia.edu

Samantha L. Gorman
Dept. of Biomedical Engineering
Columbia University
New York, NY USA
slg2186@columbia.edu

Daniella A. Jimenez
Dept. of Biomedical Engineering
Columbia University
New York, NY USA
dj2357@columbia.edu

Elisa E. Konofagou
Dept. of Biomedical Engineering
Dept. of Radiology
Columbia University
New York, NY USA
ek2191@columbia.edu

Abstract—Focused ultrasound-mediated blood - brain barrier opening has been proven to be a safe, noninvasive, and transient method for neurological treatment. The method was initially proposed for drug delivery; however, recent work has highlighted neuroimmunotherapeutic stimulation observed through neurodegenerative disease related pathology reduction in addition to cognitive benefits, particularly among murine Alzheimer’s disease models. Previous studies have indicated a potential relationship between the gut microbiome and Alzheimer’s disease proliferation. In this study, we sought to investigate the effects of focused ultrasound blood - brain barrier opening on the gut microbiome of 3xTg mice. In the study herein, we present evidence of focused ultrasound blood - brain barrier opening induced changes in the gut microbiome of mice, indicating normalization of AD microbiome to that of a wildtype mouse as well as increased alpha diversity among control mice.

Keywords—Focused ultrasound, Blood-brain barrier opening, Alzheimer’s disease, microbiome

I. INTRODUCTION

Focused ultrasound blood - brain barrier opening (FUS - BBBO) is a safe, noninvasive, and transient method of opening the blood brain barrier when combined with intravenously injected microbubbles (MB) [1]. Initially considered as a method for drug delivery, FUS has also shown promise as a neuroimmunotherapeutic method through reduction of Alzheimer’s disease (AD) protein histopathology and improved cognitive benefits as shown in AD murine models [2].

AD is known to be a major cause of dementia and accounts for 60 - 70% of all dementia cases [3]. Observed at a higher rate among women, it is an incapacitating disorder affecting

individuals in a variety of ways from memory loss to lacking motor function. Some factors influencing the disease include age, immune system dysfunction, and genetic factors such as mutations of the amyloid precursor protein (APP) [4].

Previous work has indicated that the gut microbiota, an ecological community of microorganisms living symbiotically and pathogenically within the body, have an impact on the synthesis of various neurotransmitters and neuromodulators [3]. Consequently, gut - brain communication via the gut - brain axis and cerebral function are affected. Moreover, other studies have found that the microbiota of aged, Alzheimer’s disease affected individuals have a lower level of bacteria, resulting in decreased butyrate levels and increased inflammation of the brain and as well as the progression of cognitive loss [3].

Additionally, it has been shown that the AD development may start in the gut and spread to the brain as the translocation of AB oligomers from the intestine to the brain was observed [5]. As a result, this highlights the critical role of the microbiome in neurodegeneration. Thus, we sought to investigate the effect of FUS - BBBO on the murine microbiome. In this study, we present novel evidence demonstrating the effect of FUS-BBBO on altering the gut microbiome in AD, emphasizing the peripheral effects associated with FUS - BBBO.

II. MATERIALS AND METHODS

A. Animal Use

The animals used in this study were housed and handled accordingly with Columbia University’s Institutional Care and Use Committee under protocol #AC - AABG559. Female, twelve - month old triple transgenic (3xTg) mice were used for their ability to mimic proliferation of pathology in human Alzheimer’s disease. This model is achieved through the co-injection of human APP_{Swe} and tau_{p301L} into a PS1_{M1146B} knockin

mouse model such that human amyloid and tau pathology as well as synaptic dysfunction are represented [6]. Age matched, wild - type mice were also used in the study. The groups studied in this work were the following: WT sham, WT FUS - BBBO, AD sham, and AD FUS - BBBO where sham mice were introduced only to anesthesia.

B. Focused Ultrasound Blood – Brain Barrier Opening

FUS-BBBO was performed using parameters previously established in efficacy and safety studies [7]. Mice were anesthetized with 2% isoflurane for the duration of the session (SurgiVet, Smiths Medical PM, Inc., Dublin, OH, USA). Their heads were fixed in a stereotactic frame (David Kopf Instruments, Tujunga, CA, USA). Hair removal of the head took place through electric razor and depilatory cream to reduce impedance mismatch. Degassed ultrasound coupling gel was placed on the head followed by the placement of a water bath over the subject’s head. A 3D positioning system (Velmex Inc., Lachine, QC, Canada) was used to move the transducer over the lambdoid suture of the skull. Here, a single - element, spherical-segment FUS transducer (f_c : 1.5 MHz, focal depth: 60 mm, radius: 30 mm Imasonic, France) was driven by a function generator (Agilent, Palo Alto, CA, USA) via a 50 - dB power amplifier (E&I, Rochester, NY, USA). This set - up was used for treatment of the bilateral hippocampus. A single - element transducer (center frequency: 10 MHz, focal depth: 60 mm, radius 11.2 mm; Olympus NDT, Waltham, MA, USA) was aligned at the center of the concave FUS transducer for passive cavitation detection (PCD) of real - time microbubble activity during sonication. The PCD was driven by a pulser/receiver (Olympus, Waltham, MA, USA) and connected to a digitizer (Gage Applied Technologies, Inc., Lachine, QC, Canada). The FUS setup is illustrated in Fig. 1.

Bilateral hippocampal control sonications occurred for 60s at 450 kPa where baseline cavitation was performed first, followed by that of experimental conditions. When utilized, lipid - shelled, in-house, customized polydisperse microbubbles were injected intravenously between baseline and experimental sonications through a bolus of 3 μ L MB diluted in 100 μ L sterile saline (8×10^8 /mL, mean diameter: 1.4 μ m) [8]. All relevant parameters are provided in Table I.

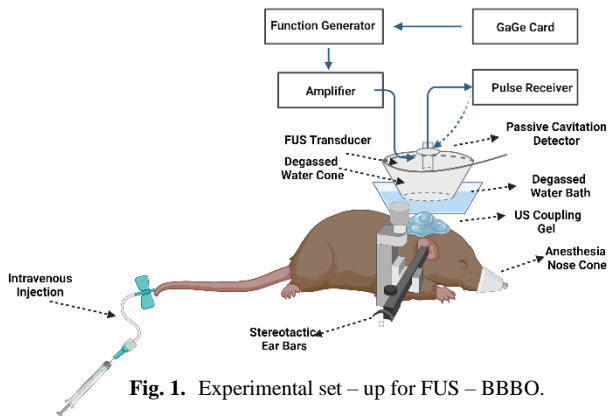


Fig. 1. Experimental set – up for FUS – BBBO.

TABLE I. FUS Parameters.

FUS Parameters		
FUS Transducer	Center Frequency	1.5 MHz
	Focal Length	60 mm
	Radius	30 mm
	Peak Negative Pressure	450 kPa
	Sonication duration	60 sec/target
Passive Cavitation Detector	Center Frequency	10 MHz
	Focal Depth	60 mm
Microbubbles	In – house made	Polydisperse (mean diameter: 1.4 μ m)
	8×10^8 MB/mL	100 μ L bolus injection

C. Magnetic Resonance Imaging

Confirmation of FUS - BBBO encompassed imaging with a 9.4T MRI system (Bruker Medical, Boston, MA). Mice received an intraperitoneal injection of 0.2 mL of gadodiamide (OmniscanTM, GE Healthcare, Princeton, NJ, USA), which does not diffuse through the intact BBB. Imaging was performed using a contrast - enhanced 2D FLASH sequence (TR/TE 230/3.3 ms, flip angle: 70°, number of excitations: 6, field of view: 25.6 mm \times 25.6 mm).

D. Fecal Collection and Analysis

Fecal samples (3 dropping per mouse) were collected at baseline before treatment and 24 hours post - treatment and stored -80 °C. 16s rRNA sequencing was performed on all fecal samples for identification of bacterial populations and classification of the microbiome. Manual extraction took place with DNA Extraction positive control: ZymoBIOMICS Microbial Community Standard (D6300) and Extraction Kit: DNeasy PowerSoil Pro Kit (Catalog# 47016). The sequencing method applied was V3 – V4 with Illumina NXTR[®] XT IDDX Kt v2 MiSeq 2x300. Interpretation, statistical analysis, and visualization were performed using R with the phyloseq and metacoder packages in addition to GraphPad Prism. The experimental timeline is illustrated in Fig 2.

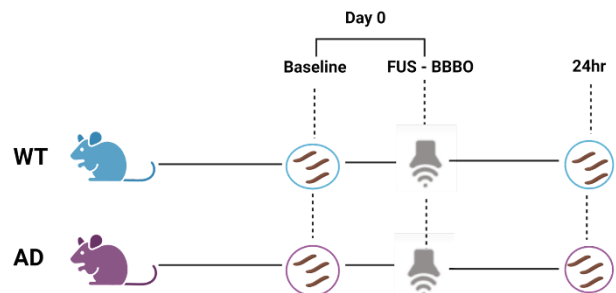


Fig. 2. FUS – BBBO parameters used for the sonications conducted for the respective mice in this study.

III. RESULTS

A. Overview of gut microbiota composition

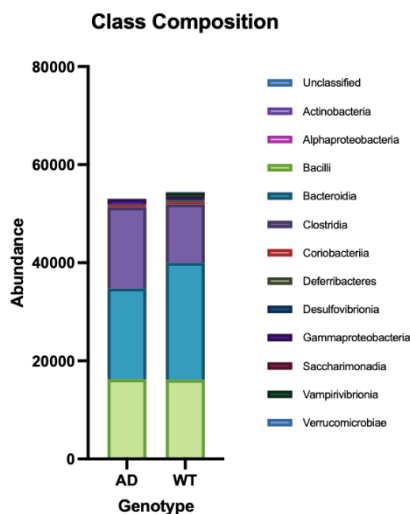


Fig. 3. Abundance of representative families found in fecal samples of WT and AD mice. Each component of the cumulative bar chart indicates a family with the size correlating to abundance levels.

Out of the 24 fecal samples examined, a total of 2,845 16S RNA sequences were identified. These sequences were organized into 113 operational taxonomic units (OTUs) and categorized into nine distinct phyla. These overarching groups were further subdivided into 13 bacterial families. The predominant families present in both the AD and WT genotypes included Bacilli, Bacteroidia, and Clostridia. Notably, Deferribacteres were entirely absent from the AD samples (Fig. 3). Interestingly, AD mice exhibited a higher abundance of Clostridia and Bacilli, whereas Bacteroidia levels were diminished.

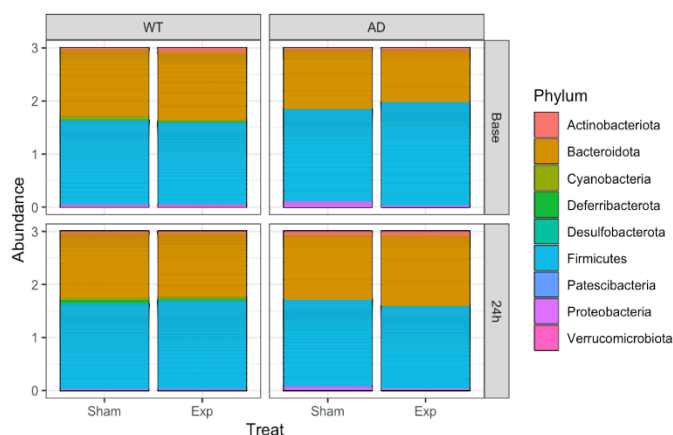


Fig. 4. FUS-BBBO alters murine gut microbiome relative abundance 24 hours post treatment. Bar plot depicting differences in relative Phylum abundance 24 hours post FUS-BBBO treatment in WT and AD groups.

B. Microbiota differences 24 hours post FUS – BBBO

To examine the impact of FUS-BBBO on the murine gut microbiota, we analyzed differences in phylum abundance across the various groups. Both the WT and AD sham groups demonstrated minimal variation in phylum abundance from the baseline to the 24-hour timepoint (Fig. 4). Notably, AD mice displayed the most substantial response to FUS, exhibiting changes of an average of 9.36% in the Bacteroidota phylum and -9.70% in the Firmicutes phylum. In comparison, WT mice showed average changes of -8.29% and 7.79% in the Bacteroidota and Firmicutes phyla, respectively. Among AD experimental mice, Actinobacteria and Proteobacteria exhibited smaller changes of 1.29% and -1.07%, respectively; however, these changes were below 1% in WT mice (Fig. 5). For all other phyla, changes were also below 1% at the 24-hour mark following FUS-BBBO.

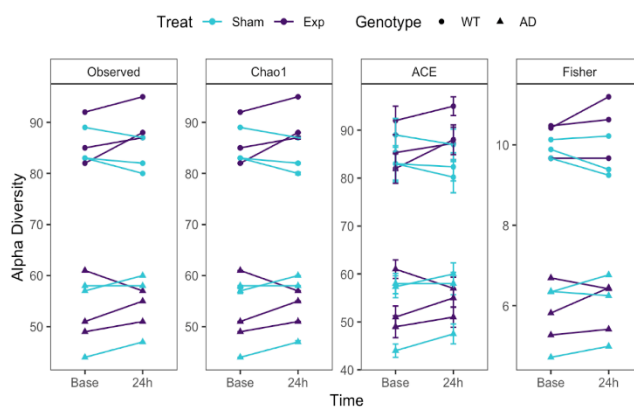


Fig. 5. The scatter plot displayed quantifies differences in Actinobacteria, Bacteroidota, Firmicutes, and Proteobacteria in WT and AD baseline groups from AD experimental group 24 hours after treatment.

The alpha diversity of each sample was assessed both at baseline and the 24-hour timepoint, utilizing four distinct indices for analysis (Fig. 6). Notably, WT samples exhibited a more diverse microbiota community when contrasted to AD samples. After FUS-BBBO treatment, there was an observable increase in alpha diversity in WT samples. Among the AD groups, in both the sham and FUS cohorts, there was a general increase at the 24-hour timepoint, with the exception of one experimental mouse that displayed a decrease across all indices.

IV. DISCUSSION

This study presented herein uncovered a normalization in the relative abundance of core phyla within AD (3xTg) mice following FUS-BBBO. This normalization is characterized by lower or higher numbers of Firmicutes and Bacteroidota, respectively. These shifts closely mirror the baseline levels observed in age-matched control wildtype mice. Additionally, these changes align with findings from previous studies in AD mouse models, which also demonstrated a lower relative abundance of Bacteroidota and a higher relative abundance of Firmicutes compared to control mice [9,10].

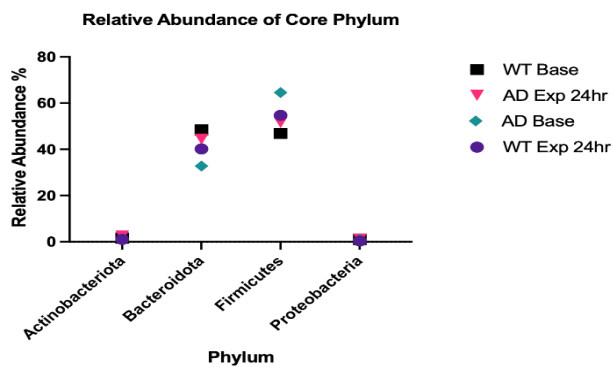


Fig. 6. Alpha Diversity Richness Plot Comparing Changes from Baseline to 24 Hours Post-FUS-BBBO. Observed species index reflects total number of species within the sample (n = 3 mice per treatment group for AD and WT genotypes). Chao1 index accounts for the number of rare species that were singletons or doubletons to estimate the total number of species in the community. Ace index estimates species richness by considering the number of rare species in the community. Fisher Alpha index quantifies the evenness or unevenness in the distribution.

Moreover, when considering fecal microbiota transplantation from wildtype to AD mice, cognitive deficits and neurodegeneration were alleviated, accompanied by an increase in the relative abundance of Bacteroidota [5]. However, it is important to note that there exists conflicting evidence regarding the effects of these different phyla in the context of healthy aging and neurodegenerative diseases [11,12,13].

Our findings also indicate a rise in alpha diversity among wild-type mice. Notably, prior research has highlighted a reduction in alpha diversity in both AD patients and AD mouse models [13,14]. This work corroborates with lower alpha diversity in AD, but intriguingly, this decreasing pattern was not observed in 3xTg animals. This suggests that the effects of FUS-BBBO on the microbiome might differ between healthy and pathological states.

Supporting this notion, our research group has previously demonstrated that aging and AD affect the opening volumes and closing kinetics of FUS-BBBO in mice [15]. Nevertheless, it is important to acknowledge the limitations of our pilot study, including the small number of animals involved and the relatively short observation period.

V. CONCLUSION

For the first time, the study presented herein demonstrates the effects of FUS - BBBO on the microbiome in wildtype mice and in a murine model of Alzheimer's Disease. FUS-BBBO has been reported to alert microglia and peripheral macrophages in the brain that can subsequently reduce beta amyloid and tau loads. Peripheral macrophages may also subsequently affect other linked organs. Our results reveal potentially beneficial peripheral effects of FUS-BBBO through changes in the microbiome which have been implicated in the pathogenesis of a variety of neurodegenerative diseases. The results also show that the systemic benefits of FUS-BBBO

outside the brain. Further studies are necessary to investigate the mechanism of action, long-term effects and the detailed contribution of different species in the microbiome.

ACKNOWLEDGMENTS

The study was funded in part by the National Institutes of Health (R01 AG038961). The authors acknowledge BioRender for some graphics created and included in this work.

REFERENCES

- [1] A. R. Kline-Schoder, R. L. Noel, H. Phatnani, V. Menon, and E. E. Konofagou, "Focused ultrasound-mediated blood-brain barrier opening best promotes neuroimmunomodulation through brain macrophage redistribution," *Neuroglia*, vol. 4, no. 2, pp. 141–157, 2023. doi:10.3390/neuroglia4020010
- [2] M. E. Karakatsani *et al.*, "Focused ultrasound mitigates pathology and improves spatial memory in alzheimer's mice and patients," *Theranostics*, vol. 13, no. 12, pp. 4102–4120, 2023. doi:10.7150/thno.79898
- [3] A. Megur, D. Baltrikienė, V. Bukelskienė, and A. Burokas, "The microbiota-gut-brain axis and alzheimer's disease: Neuroinflammation is to blame?," *Nutrients*, vol. 13, no. 1, p. 37, 2020. doi:10.3390/nu13010037
- [4] C. Sala Frigerio *et al.*, "The major risk factors for alzheimer's disease: Age, sex, and genes modulate the microglia response to AB plaques," *Cell Reports*, vol. 27, no. 4, 2019. doi:10.1016/j.celrep.2019.03.099
- [5] Y. Sun *et al.*, "Intra-gastrointestinal amyloid- β 1-42 oligomers perturb enteric function and induce alzheimer's disease pathology," *The Journal of Physiology*, vol. 598, no. 19, pp. 4209–4223, 2020. doi:10.1113/jp279919
- [6] R. L. Noel, S. L. Gorman, A. J. Batts, and E. E. Konofagou, "Getting ahead of alzheimer's disease: Early intervention with focused ultrasound," *Frontiers in Neuroscience*, vol. 17, 2023. doi:10.3389/fnins.2023.1229683
- [7] E. E. Konofagou, "Optimization of the ultrasound-induced blood-brain barrier opening," *Theranostics*, vol. 2, no. 12, pp. 1223–1237, 2012. doi:10.7150/thno.5576
- [8] J. A. Feshitan, C. C. Chen, J. J. Kwan, and M. A. Borden, "Microbubble size isolation by differential centrifugation," *Journal of Colloid and Interface Science*, vol. 329, no. 2, pp. 316–324, 2009. doi:10.1016/j.jcis.2008.09.066
- [9] H.-J. Lee, K.-E. Lee, J.-K. Kim, and D.-H. Kim, "Suppression of gut dysbiosis by Bifidobacterium Longum alleviates cognitive decline in 5xfad transgenic and aged mice," *Scientific Reports*, vol. 9, no. 1, 2019. doi:10.1038/s41598-019-48342-7
- [10] E. Sanguinetti *et al.*, "Microbiome-metabolome signatures in mice genetically prone to develop dementia, fed a normal or Fatty Diet," *Scientific Reports*, vol. 8, no. 1, 2018. doi:10.1038/s41598-018-23261-1
- [11] J. Sun *et al.*, "Fecal microbiota transplantation alleviated alzheimer's disease-like pathogenesis in APP/PS1 transgenic mice," *Translational Psychiatry*, vol. 9, no. 1, 2019. doi:10.1038/s41398-019-0525-3
- [12] M. J. Claesson *et al.*, "Composition, variability, and temporal stability of the intestinal microbiota of the elderly," *Proceedings of the National Academy of Sciences*, vol. 108, no. supplement_1, pp. 4586–4591, 2010. doi:10.1073/pnas.1000097107
- [13] N. M. Vogt *et al.*, "Gut microbiome alterations in alzheimer's disease," *Scientific Reports*, vol. 7, no. 1, 2017. doi:10.1038/s41598-017-13601-y
- [14] E. M. Borsom *et al.*, "A longitudinal study of the unique gut microbiota of 3xTg-AD mice modeling key AD pathologies," *Alzheimer's & Dementia*, vol. 17, no. S3, Feb. 2022. doi:https://doi.org/10.1002/alz.054633
- [15] R. L. Noel *et al.*, "Natural aging and alzheimer's disease pathology increase susceptibility to focused ultrasound-induced blood-brain barrier opening," *Scientific Reports*, vol. 13, no. 1, 2023. doi:10.1038/s41598-023-30466-6